Natural Hazards
https://doi.org/10.1007/s11069-024-06848-y

ORIGINAL PAPER

Which droughts are becoming more frequent? A copula entropy analysis on the return period of droughts in Europe

Pedro H. L. Alencar[1] · **Eva N. Paton**[1]

Received: 6 November 2023 / Accepted: 24 July 2024

Abstract
Climate change and global warming have increased the frequency of extreme events, particularly over the past decades. Changes in drought frequency are not yet understood, especially regarding which drought features are becoming more frequent (e.g., are longer or high-magnitude droughts becoming more frequent, or both?). In this study, we present a novel methodology to accurately and consistently estimate changes in return periods of different types of droughts. For this purpose, we implemented copula-entropy theory to assess drought frequencies and their changes. As an example of the application of the proposed method, we used data from the European Climate Assessment and Dataset (ECA&D), from which we selected 26 stations in Central Europe with over 100 years of data and low incidence of missing days ($\leq 0.3\%$). The results of the new analysis indicate that there was a high variability in the frequency change patterns across Central Europe over the last century; however, most regions have experienced an increase in the frequency of medium-to-high intensity droughts. The use of the copula-entropy theory to assess drought frequency is a reliable method that allows systematic monitoring and easy updating of current knowledge, and is computationally efficient and statistically robust.

Keywords Drought · Copula theory · Entropy theory · Climate change

1 Introduction

Droughts represent a significant a threat arising from climate change by disrupting water, food, and energy supplies (Teutschbein et al. 2023). Studies have suggested that the frequency of droughts has increased over the past century, particularly within the last five decades (Wuebbles et al. 2017; Cai et al. 2021; Gül et al. 2021). Moreover, in all greenhouse gas emission scenarios, extreme events, such as droughts, are expected to become more frequent in the coming decades (Spinoni et al. 2017; Wuebbles et al. 2017). The latest

✉ Pedro H. L. Alencar
pedro.alencar@campus.tu-berlin.de

Eva N. Paton
eva.paton@tu-berlin.de

[1] Chair of Ecohydrology, Institute of Ecology, Technical University of Berlin, Ernst-Reuter-Platz, 1, 10578 Berlin, Germany

IPCC report (IPCC 2023) highlights that the younger generations are likely to experience a significantly higher frequency of droughts, up to four times more often than in the pre-industrial era (Thiery et al. 2021).

While a universally applicable definition of drought proves challenging (Lloyd-Hughes 2013), droughts are generally characterised by prolonged periods of abnormally dry weather that cause significant hydrological imbalances (WMO 1992). Mishra and Singh (2010) categorised droughts into four types based on their effects on populations and ecosystems: meteorological, hydrological, agricultural, and socioeconomic droughts. However, this framework is not exhaustive (Crausbay et al. 2020). With the evolving climate, new drought classifications of droughts have emerged, encompassing phenomena such as flash droughts (Alencar and Paton 2022), snow droughts (Mote et al. 2016), human-induced and -modified droughts (Loon et al. 2016), anthropogenic droughts (AghaKouchak et al. 2021), and mega droughts (Cook et al. 2016).

Various types of drought and their respective categories are frequently described using one or more drought indices (Svoboda et al. 2016). These indices play a crucial role in identifying such events within historical climate data or projections, particularly when impact reports are unavailable (Sheffield et al. 2012). Percentiles, anomalies, and standardised indeces are examples of these indices that deliver essential insights into drought characteristics for managers and decision-makers, thus facilitating preparedness (Cravens et al. 2021). After establishing a set of criteria for identifying specific drought categories (Svoboda et al. 2002; Zink et al. 2016), it is possible to envision the characteristics of droughts with specific *return periods* (e.g. $T_r = 100$ years). This concept is frequently employed in the design of hydraulic structures, such as channels, drainage systems, and reservoirs, offering valuable insights for devising strategies to mitigate the escalating impact of droughts (AghaKouchak 2014).

Despite the importance of understanding drought features and their return periods, most studies have not consider the multivariate nature of droughts and their recurrence times (Houmma et al. 2022). Studies that address drought return periods and specifically their changes over time often focus solely on one drought feature at a time and employ short temporal series Spinoni et al. 2017; Cai et al. 2021; Qi et al. 2022. However, this approach is insufficient for the proper assessment of drought return periods considering the relational behaviour and statistical dependencies of duration, magnitude, and intensity (AghaKouchak 2014). The copula theory has emerged as a solution for multivariate distributions with statistically dependent marginals (Sklar 1959; Pandey et al. 2023).

The copula theory has found applications in the study of co-dependence in multivariate processes across various fields, including risk management, economics, climatic, and hydrological modelling (Hofert et al. 2019). In recent years, copulas have gained popularity for analyzing extreme and compound climatological events (Bevacqua et al. 2017; Singh and Zhang 2018; Zscheischler et al. 2020). However, previous studies focusing on assessing magnitude-duration-frequency (MDF) curves using copulas mostly relied on shorter datasets and precipitation-based indices Xu et al. 2015; Tosunoglu and Can 2016; Ayantobo et al. 2018; Hasan and Abdullah 2022. Moreover, selecting an appropriate probability distribution and copula functions involves testing multiple "candidate" functions and evaluating their goodness of fit (She et al. 2015; Bevacqua et al. 2017; Hasan and Abdullah 2022; Pandey et al. 2023). This process is computationally demanding, given the numerous possible candidates for each analysed station or grid point (Mikosch 2006; Zhang and Singh 2019; Hofert et al. 2019 Furthermore, this systematic search introduces uncertainty regarding whether the selected function and its parameters are the most suitable for the data (Singh 1998).

This issue has been addressed in previous studies by AghaKouchak (2014) and Singh and Zhang (2018), who studied the magnitude-duration-frequency of floods using copulas. To circumvent this issue, the authors employed the principle of maximum entropy (POME) to assess the appropriate copula and marginal distributions. Proposed by Jaynes (1957a, 1957b) the POME "provides the most unbiased representation of our knowledge of the state of the system" (Jaynes 1957a). Thus, the POME offers an evaluation of the (unknown) underlying distribution that best reflects our knowledge (and uncertainty) of the studied variables (Cover and Thomas 2006; Zhang and Singh 2019). More recent works Yang et al. 2021; Shekari et al. 2023; Wei and Zhao 2024 successfully implemented copula-entropy method for drought analysis in Iran and China, obtaining more accurate distributions in comparison to parametric copula. The application of copula-entropy to study changes in droughts in Central Europe was not carried out yet. Another novelty of this work is the use of long (over one hundred years) time series to assess not only the distribution of drought occurrence, but also its changes over the past century. Additionally, this work provides complete reproducible datasets and scripts that will allow the community to easier transfer and implement copula-entropy to other regions.

The objectives of this research are to propose a using copula-entropy for evaluating the temporal changes of MDF curves and to apply this method to assess these changes across Europe using high-quality station data over the last 100 years. To accomplish this, we developed the innovative copula-entropy-based method for deriving MDF curves, implemented as a software package named Copula-Entropy Drought Analysis in R (`cedaR`—see Declarations for more information). The `cedaR` package was subsequently used to analyse data spanning from 1920 to 2019 at various intervals, allowing an examination of how MDF curves have evolved over the decades.

2 Datasets and methods

2.1 Climate data

Historical climatic data were acquired from the European Climate Assessment & Dataset Project (ECA&D) (https://www.ecad.eu— Tank et al. 2002). The ECA&D database encompasses extensive data from more than fifteen thousand stations dispersed across Europe and the Mediterranean. In this study, we selected stations with gaps of less than 0.3% in temperature and precipitation data over the period from 1920 to 2019. Of the available stations, only 26 in Central Europe met these criteria. For these stations, gaps were filled with the closest stations with available data. The selected stations are situated across eight Central European countries: Austria, Croatia, France, Germany, Hungary, the Netherlands, Sweden, and Switzerland. They are notably concentrated in the Alps, particularly along the borders of Germany, Switzerland, and Austria (see Fig. 1). A comprehensive list containing the stations' details is provided in the Appendix A at the end of this article.

2.2 Definition of drought

To derive the MDF distributions of droughts, a series of annual drought events was identified for each station. In this study, we employed the Standard Precipitation Evapotranspiration Index (SPEI—Vicente-Serrano et al. 2010) with a three-month accumulation period (SPEI3), which is often associated with agricultural droughts (Mishra and

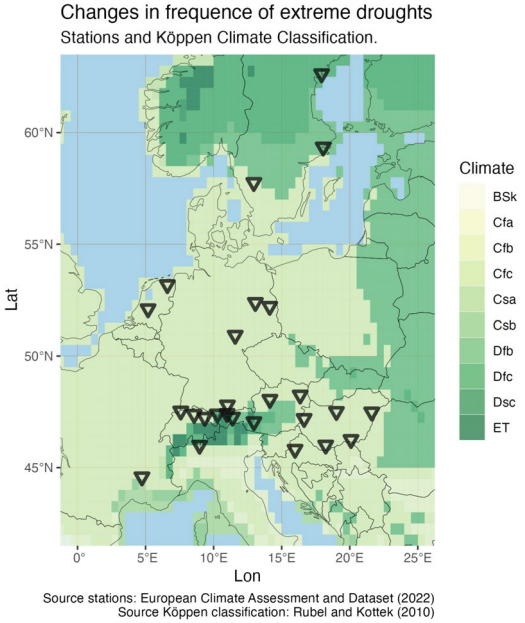

Fig. 1 Locations of the 26 selected stations and respective Köppen climate classifications. All selected stations have at least 100 year-long series of rainfall and temperature with less than 0.3% missing days

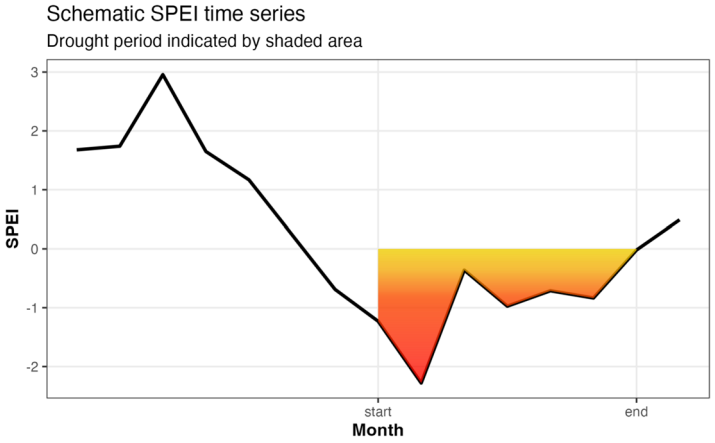

Fig. 2 Schematic drought definition. Duration is computed as the number of months with SPEI below zero after onset. Magnitude is the sum of the absolute values of SPEI throughout the drought period

Singh 2010). Droughts were defined as consecutive months characterised by negative SPEI3 values. The onset of a drought was identified by SPEI3 ≤ -1 (Vicente-Serrano et al. 2010). Based on AghaKouchak (2014), in this study, we represented the duration (D) of a drought as the number of subsequent months with negative SPEI3 values, and the magnitude (M) was quantified as the absolute sum of SPEI over the duration of a drought ($M = \sum_{i=\text{start}}^{\text{end}} \text{abs}(SPEI_3)$); that is, the sum of the monthly drought index over the duration of the droughts, as depicted in Fig. 2. Additionally, a recuperation phase of

1 month is allowed (Wang et al. 2019). This means that for a drought to be considered over, SPEI3 has to be positive for at least two consecultive months.

The derived frequency (F) of droughts is the annual frequency, that is, the number of times a specific event is expected to occur annually. This frequency measure is directly linked to the definition of the return period (T_r), which is the expected time for an event to be matched or exceeded. In this study, we refer to droughts with high durations and/or magnitudes as more extreme than those with shorter duration or lower magnitude (milder droughts), that are also more frequent (Xu et al. 2019).

2.3 Copula-entropy theory

A copula-entropy approach was used to derive MDF curves for droughts using the most entropic canonical copula method (MECC) following Singh and Zhang (2018). The MECC represents a specific type of parametric copula (Nelsen 2007) and is also the simplest form (i.e. canonical; Jeffreys, 2000; Chu and Satchell, 2018) of a copula function that maximises the system's entropy (Zhang and Singh 2019). Utilising the MECC allows us to circumvent the complex and computationally demanding task (Mikosch 2006) of searching for the most suitable copula (She et al. 2015; Pandey et al. 2023). The MECC is derived by maximising the entropy (H) of the copula distribution (c) while adhering to a set of constraints. For the bivariate scenario, the entropy of the copula distribution can be expressed as:

$$H(u,v) = -\int_{\Omega} c(u,v)\ln c(u,v)\,\mathrm{d}u\mathrm{d}v \tag{1}$$

where u and v are the marginals (studied variables). By definition (Sklar 1959), copula marginals are restricted to the interval [0, 1]. Ω is the space of integration, equivalent to the interval $[0,1]^2$. Equation (1) was maximised using the Lagrangian multipliers method, as recommended by Singh and Zhang (2018), with assistance of the Nelder-Mead Simplex method (Lagarias et al. 1998). The maximisation problem presented in Eq. (1) has the following contranis (Eq. 2):

$$\kappa_0 : \int_{\Omega} c(u,v)\mathrm{d}u\mathrm{d}v = 1 \tag{2a}$$

$$\kappa_1 : \int_{\Omega} uc(u,v)\mathrm{d}u\mathrm{d}v = E(U) = \frac{1}{2} \tag{2b}$$

$$\kappa_2 : \int_{\Omega} u^2c(u,v)\mathrm{d}u\mathrm{d}v = E(V) = \frac{1}{3} \tag{2c}$$

$$\kappa_3 : \int_{\Omega} vc(u,v)\mathrm{d}u\mathrm{d}v = E(U^2) = \frac{1}{2} \tag{2d}$$

$$\kappa_4 : \int_{\Omega} v^2c(u,v)\mathrm{d}u\mathrm{d}v = E(V^2) = \frac{1}{3} \tag{2e}$$

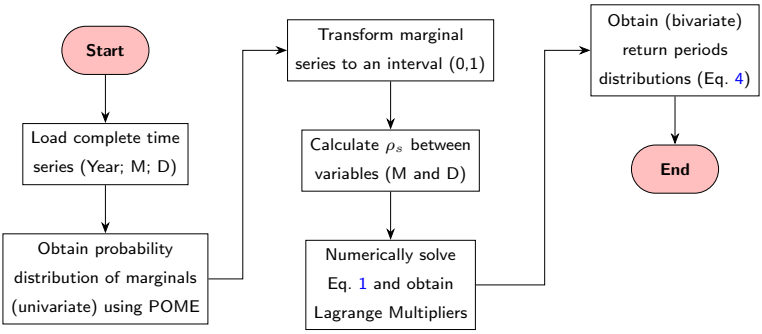

Fig. 3 Workflow to obtain the joint probability distribution of Magnitude (M)–Duration (D) using copula-entropy theory and to assess return periods of events. ρ_s is Spearman's rank correlation

$$\kappa_5 : \int_{\Omega} uvc(u,v)\mathrm{d}u\mathrm{d}v = \frac{\rho_s + 3}{12} \tag{2f}$$

where κ_i are the constrains to the maximization of Eq. (1). κ_0 (Eq. 2a) is the trivial constraint that applies to all distributions, signifying that the total sum equals one. Constraints κ_1 through κ_4 pertain to the marginal distributions, while κ_5 represents a measure of dependence. The Spearman's rank correlation coefficient (ρ_s) was employed as the dependence measure, following the approach suggested by AghaKouchak (2014), and Singh and Zhang (2018).

Copula-based definition of return period

In this study, we analysed the bivariate case of the MECC of drought frequencies, using the distributions of the duration and magnitude of droughts (Eq. 3). To assess the return period of droughts (T_r), we use the additive (Boolean "and") return period, where both variables must be exceeded, that is, $U > u$ and $V > v$ (Eq. 4).

$$\int_0^u \int_0^v c(u,v)\mathrm{d}u\mathrm{d}v = C(u,v) = C[P(\text{duration}), Q(\text{magnitude})] \tag{3}$$

where P and Q are the cumulative distribution functions of the marginals (magnitude and duration, respectively).

$$T_r = \frac{1}{1 - u - v + C(u,v)} \tag{4}$$

2.4 Copula-entropy drought analysis workflow

To derive the MDF distributions, we employed the functions implemented in the `cedaR` package, following the systematic workflow depicted in Fig. 3. Once a series of drought events, including their magnitude and duration, was obtained based on the definition in Sect. 2.2, we computed the probability distribution of the marginal distributions using the POME (Singh 1998; Alencar et al. 2021). Subsequently, we transformed the marginals into open intervals (0, 1), a requirement in copula theory (Chu and Satchell 2018), and calculated the Spearman's rank correlation coefficient, which is one of the constraints for the

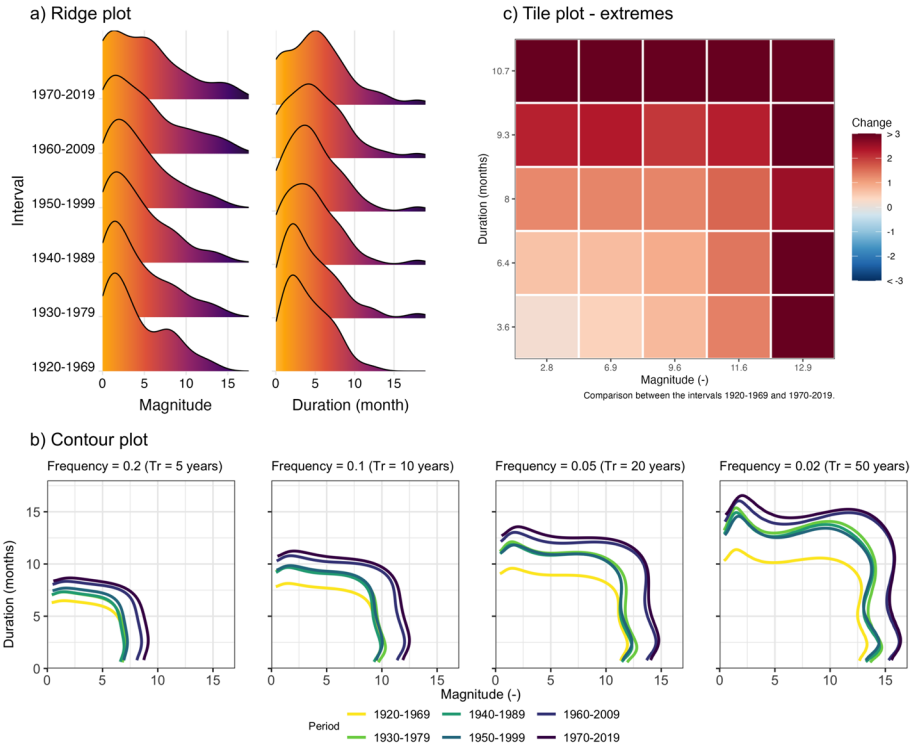

Fig. 4 Visualization of the four-dimensional framework (duration, magnitude, frequency, and time). **a** Changes in each of the individual features (duration, magnitude, and frequency) over the decades. Each ridge is obtained with 50 years of continuous data. **b** Tile plot with the change in frequency of different combinations of magnitude and duration. **c** Contour plots indicating the change in the combined values of magnitude and duration over the decades in a continuous progression

entropy maximisation (Eq. 2f). Maximising Eq. (1) yields the Lagrange multipliers needed to define the copula distribution (C—Eq. 3), which, in turn, was utilised to derive the return periods of the droughts and the corresponding MDF curves (Eq. 4).

The workflow shown in Fig. 3 was implemented as a new package entitle entitled `cedaR`. The package (Alencar 2023), contains all necessary functions to obtain the MECC distribution for the variables of interest (bivariate) and return period distributions, as well as a comparison of the changes in those distributions and visualisation tools. It can also be used with other drought indeces in addition to SPEI.

2.5 Drought change visualisation

Visualising changes in drought frequency with respect to multivariate analysis is a challenge, as we must to display these changes in a four-dimensional framework considering duration, magnitude, frequency, and time. In this study, we proposed the use of three different types of plots to assist in the interpretation (Fig. 4).

Multiple ridge plots (Fig. 4a) were used to perform an initial analysis of decadal shifts in the distribution of individual variables (magnitude and duration). However, ridge plots provide only limited information on how the associated magnitudes and durations change.

In the example plot in Fig. 4a, there is a visible increase in the right-side tail for both the magnitude and duration plots, with a more pronounced dislocation of the median duration value (peak of the ridge) to the right side.

The contour plots (Fig. 4b) allow the visualisation of the progressive change in the magnitude and duration of droughts with the same return period (*viridis*-coloured lines) over the decades. Each plot shows the changes in a specific return period (5, 10, 20, and 50 y) for the *pair* magnitude-duration. In this visualisation we can compare the change within the same return period value (e.g. a drought with a5-month duration and a return period of 50 years would have a magnitude of 12 in 1920–1969 and 15 in 1970–2019). It is also possible to compare changes over different return periods; for example, an event with a magnitude of 10 and a duration of 10 months would be classified as a 50-year return period in 1920–1969, but would be classified as a 20-year T_r in 1940–1989 and a 10-year T_r in 1970–2019. In addition, an intuitive interpretation of the contour plots is the overall trend of the curves within each plot. If there is an overall displacement of the curves with more recent data (darker colour) towards the upper-right corner, there was an increase in the frequency of extreme droughts (Sect. 2.2). Conversely, if the displacement is towards the bottom-left corner, there was a decrease in the frequency of extreme droughts.

Finally, in the tile plots (Fig. 4c), we display the combination of particular values of magnitude and severity chosen from the distribution of drought events in the reference period at the beginning of the last century (1920–1969), that is. the 2-, 5-, 10-, 20- and 50-year return periods. The values of the return period for the latest period (1970–2019) are computed and compared to the reference using Eq. (5). These plots could be used to analyse the changes in selected drought scenarios and easily observe changes in the occurrence of droughts with multiple combinations of magnitude and duration, including high-intensity droughts (short duration and high magnitude). Tile plots could also be a convenient tool for practitioners to assess changes in hazards and evaluate the current strategies and infrastructure developed in the past to cope with droughts (Wang et al. 2023).

$$\text{Change} = \frac{Tr_{1970-2019} - Tr_{1920-1969}}{Tr_{1920-1969}} \tag{5}$$

3 Results

Using the proposed copula-entropy analysis (`cedaR`) method, we obtained MDF curves for all selected stations (Fig. 1). Across the 26 selected stations, we analysed the univariate and bivariate changes in a four-dimentional framework (drought duration, magnitude, frequency, and time) using the three visualisation techniques (Sect. 2.5). The corresponding plots are provided in the Supplements, and a selection of typical plots are shown in the following figures. We detected three categories of how droughts have evolved over the last century: (1) a steady increase in the extremeness of droughts, leading to a reduction in the return period of very long and/or high-magnitude droughts; (2) a consistent decrease in the extremeness of droughts, resulting in an increase in the return period of very long and/or high-magnitude droughts; and (3) mixed behaviour, involving a decrease in the return period of some longer droughts while simultaneously increasing T_r for high-magnitude droughts, or vice versa. Of the 26 analysed stations in Central Europe, 14 were classified into category 1 (increase), six into category 2 (decrease) and six into category 3 (mixed

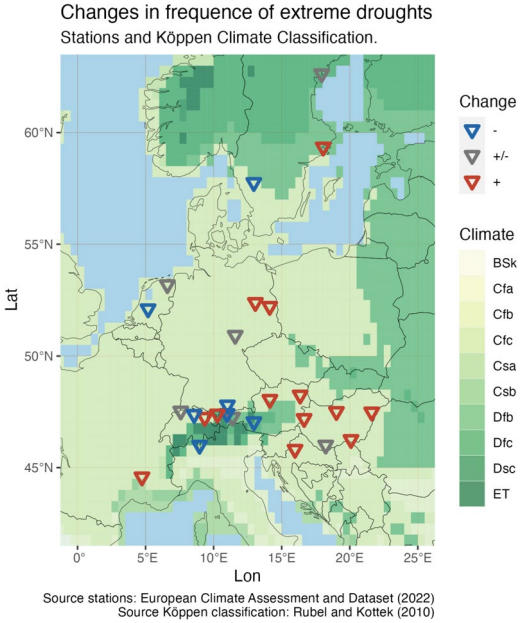

Fig. 5 Location of selected stations and their categories. Stations in category 1 are marked in red (increase), stations in category 2 are marked in blue (decrease), and stations in category 3 are marked in grey (mixed behaviour)

behaviour), as displayed in Fig. 5. The following three subsections detail the characteristics and changes in droughts of each category.

The classification of each station was based on the analysis of the three visualisation aids (Sect. 2.5) and is presented in Fig. 5[1]. A detailed list of the stations, their characteristics, and behaviours is presented in the Appendix A.

3.1 Univariate changes

In the ridge plots (Sect. 2.5), it is possible to visualise changes in the probability distributions for each individual variable. These plots also display trends in the central values and tails corresponding to an increase or decrease in the occurrence of extreme-duration/magnitude events. In Fig. 6, we present the ridge plots of the magnitude and duration of the stations Wien (Austria), Hohenpeissenberg (Germany), and Harnosand (Sweden) stations, which are examples of the three groups (increasing, decreasing and mixed behaviours).

For the station in Wien (Fig. 6a), which represents the behaviour in category 1, we observed a significant increase in the right-side tail, particularly in the magnitude distribution. A displacement in the peak of the duration distribution towards the right side was also visible, indicating that, on average, droughts have become longer at this station. Figure 6b displays the univariate change at station Hohenpeissenberg, which represents category 2 and presents a decrease in the frequency of longer and higher-magnitude droughts, as evidenced by the reduction in the right-side tail and the significant increase in the distribution peaks near the vertical axis on the left side. Finally, Fig. 6c shows the changes in the

[1] To guide the reader on the distribution of changes across the 26 stations an interactive on-line application is available (cedaR-app).

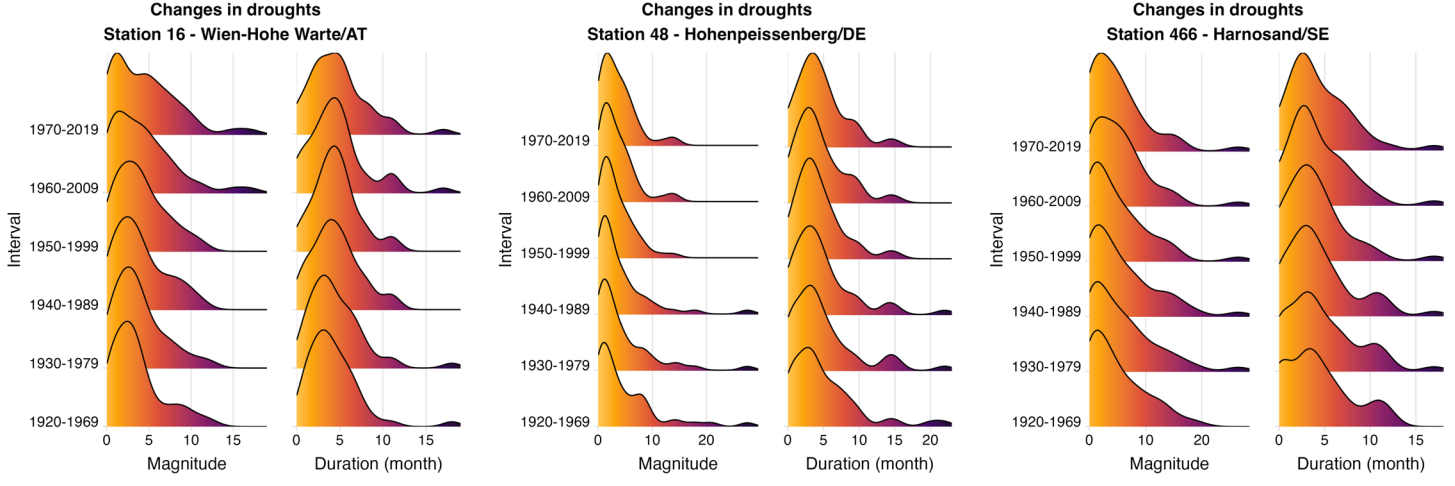

Fig. 6 Non-parametric probability density distributions of duration and magnitude for the stations in **a** Vienna (AT—category 1), **b** Hohenpeissenberg (DE—categoty 2), and **c** Harnosand (SE—category 3). Each curve was obtained using the aggregated 50-year-long time series

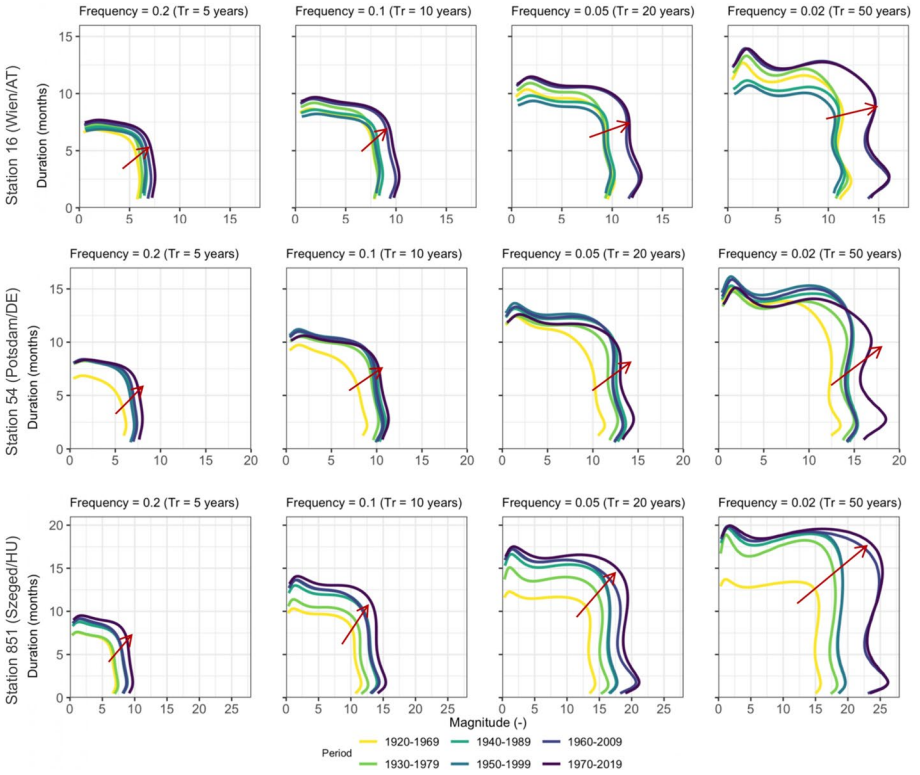

Fig. 7 Magnitude-Duration-Frequency curves for droughts with return periods of 5, 10, 20, and 50 years. Red arrows signify shifts towards more extreme droughts (i.e., longer and/or higher magnitude). Each curve is obtained from a 50-year long time series of drought occurrences. Location of stations: **a** Vienna (AT), **b** Potsdam (DE), and **c** Szeged (HU)

univariate distributions at the Harnosand Station (category 3: mixed behaviour). This station shows an increase in the right-side tail, which indicates an increase in the frequency of extreme-duration and -magnitude droughts. However, this increase is not uniform, as evidenced by the decrease in the frequency of droughts with a duration between 10 and 13 months, as well as for droughts a with magnitude of approximately 20. However, these plots do not show the co-dependencies of the changes and only provide limited insight into the actual change in the return periods of mild and extreme events.

3.2 Bi-variate changes

To visualise the co-dependencies and bi-variate changes in the return period of drought magnitude and duration, however, we use contour plots displaying changes in frequency at different values (0.2, 0.1, 0.05, and 0.02, for return periods of 5, 10, 20, and 50 years, respectively). In Fig. 7, we present three examples—Wien (Austria), Potsdam (Germany), and Szeged (Hungary)—which are part of the category 1 (14 stations that show a steady increase of frequency of extreme droughts). Figure 8 presents three examples of stations in category 2 (six stations) and shows a decrease in the frequency of extreme events: Hohenpeissenberg and Zugspize (Germany), and Zurich (Switzerland). Finally, Fig. 9 depicts

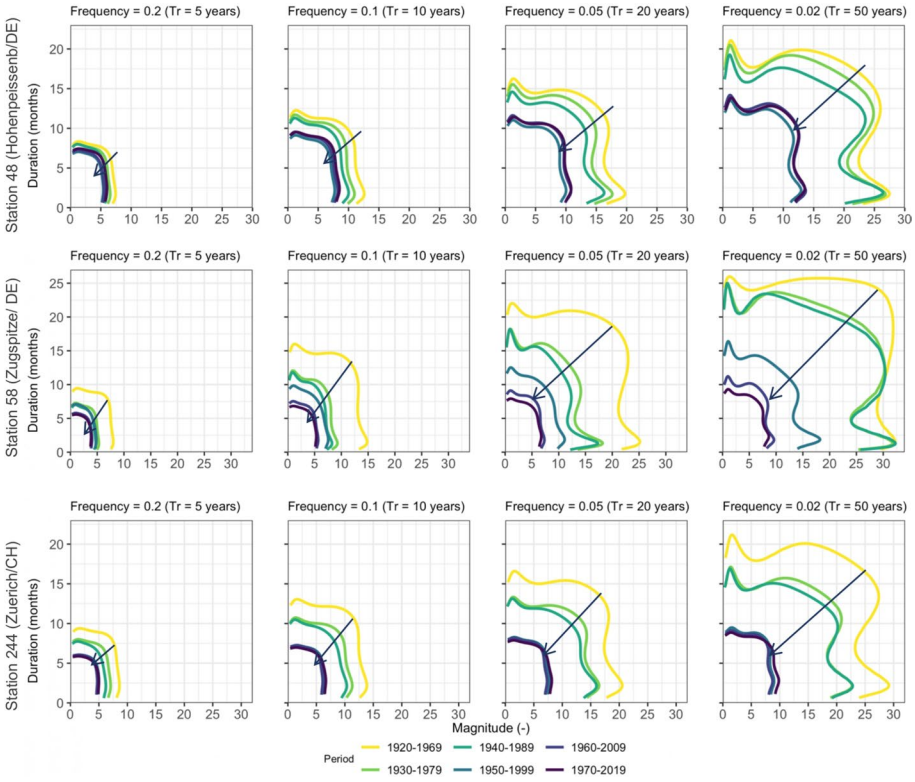

Fig. 8 Magnitude-Duration-Frequency curves for droughts with return periods of 5, 10, 20, and 50 years. Blue arrows indicate changes towards milder droughts (i.e., shorter and/or lower magnitude) under the same return period. Each curve is obtained from a 50-year long time series of drought occurrences. Location of stations: **a** Hohenpeissenberg (DE), **b** Zugspize (DE), and **c** Zurich (CH)

three examples of category 3 (six stations) that present a mixed behaviour: Harnosand (Sweden), Montelimar (France), and Lindenberg (Germany).

In Fig. 7, we present three examples of stations that are part of the category 1. For the case of the station in Wien (Austria), we observe that, for example, return periods of drought events with of magnitude 10 and 5-month duration has changed from 50 years in the period of 1920–1969 to 10 years in the most recent decades. The results for the two other stations displayed in Fig. 7 show similar trends. The station in Szeged (Hungary) exhibited an increase in both drought magnitude and duration. Additionally, the station in Potsdam (Germany) showed an particular behaviour of small change regarding the duration of events of 50-year return period while presenting a significant increase in magnitude, suggesting an increase in the intensity of more extreme droughts in the region (Schindler et al. 2007).

Figure 8 presents three examples of stations exhibited a decrease of frequency of extreme droughts (category 2). This group of six stations, as showed in Fig. 5, was mostly concentrated close to the Alps, where the literature reports a decrease in extreme drought frequency (Brunner et al 2023) and a transition to flash droughts (Yuan et al. 2023). Notably, a decrease in the occurrence of extreme droughts does not necessarily

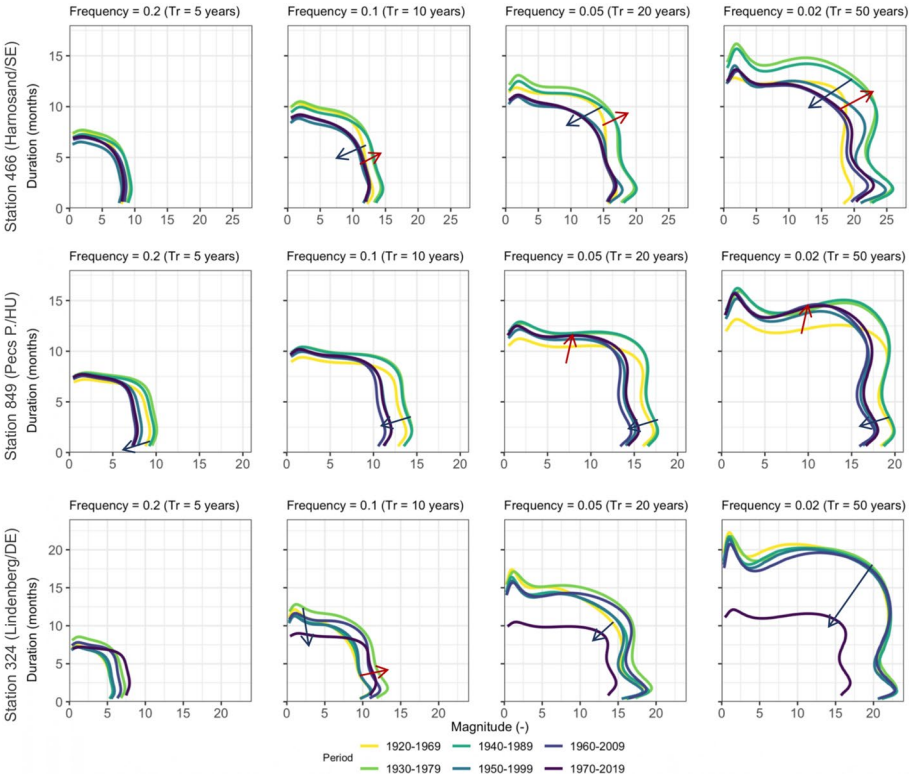

Fig. 9 Magnitude-Duration-Frequency curves for droughts with return periods of 5, 10, 20, and 50 years. Red arrows signify shifts towards more extreme droughts (i.e., longer and/or higher magnitude), while blue arrows indicate changes towards milder droughts (i.e., shorter and/or lower magnitude) under the same return period. Each curve is obtained from a 50-year long time series of drought occurrences. Location of stations: **a** Harnosand (SE), **b** Pecs Pogany (HU), and **c** Lindenberg (DE)

indicate a positive climate development in a region. This is because shorter droughts, including flash droughts, can also manifest (e.g. stations in the Alps and Sweden experienced an increase in the number of droughts). Flash droughts pose a serious threat to food production and water supply, as observed in the Alps by Brunner et al (2023) and in Spain (Noguera et al. 2020). Additionally, in our analysis, we employed the 3-month standard precipitation-evapotranspiration Index (SPEI), which, while also used to identify flash droughts, categorises them as short and mild drought events (Noguera et al. 2020).

The stations in category 3 showed a mixed behaviour regarding changes in the frequency of extreme droughts (Fig. 9). This complex and heterogeneous group included six stations located in the Netherlands, Switzerland, Hungary, and Sweden. All these stations are located in more temperate climates (Cfb) or close to climate transitions (e.g. Harnosand and Lugano). One good illustration of this group is the case of station Pecs Pogany station (Hungary), which showed a decrease in the frequency of extreme magnitudes, but an increase in duration. This indicates a transition to longer and milder droughts, particularly for higher return periods, with droughts of over 12 months (Fig. 9), which is consistent with findings in the literature (Mohammed et al 2022).

3.2.1 Changes in design scenarios

As presented in Sect. 2.5, tile plots can be used to examine the alterations in the frequency of specific combinations of drought duration and severity. This approach is particularly valuable when evaluating, for example, changes in the drought return periods relevant to the drought management infrastructure. Applying the proposed method (`cedaR`) can prove beneficial in evaluating changes in the return period of specific extreme events, such as those of exceptional duration or magnitude, and help practitioners to assess changes in the hazard to infrastructure and strategies to cope with droughts (Wang et al. 2023). Figure 10 displays the results for stations Wien (a), Hohenpeissenberg (b), and Harnosand (c) to compare the return periods for the values of duration and magnitude derived from 1920–1969.

4 Discussion

The majority of stations (14 out of 26) exhibited an increase in both the magnitude and duration of droughts, which is consistent with findings in the literature (Vicente-Serrano et al. 2022). These stations are primarily situated in oceanic or humid continental climates (Cfb and Dfb according to Köppen classification system; Rubel and Kottek, 2010) at lower altitudes. Notably, the stations in Brandenburg (Eastern Germany) and Hungary displayed an overall increase in the occurrence of extreme events, as illustrated in Fig. 5. This observed shift in the frequency of extreme droughts has also been documented in previous studies conducted in these regions (Mirschel et al 2020; Mohammed et al 2022; Vicente-Serrano et al. 2022).

Six stations have experienced a decrease in the occurrence of extreme droughts over the past century. Most of these stations are situated in regions with subarctic or tundra climates (Dfc and ET), with notable concentrations in the Alps (Switzerland, northern Italy, western Austria, and southern Germany). Among these Alpine stations, five out of nine displayed a reduction in extreme drought events. This observed decline in extreme drought frequency in the Alpine region (as depicted in Fig. 5) aligns with recent research findings that have indicated a decrease in drought duration within the same area (Brunner et al 2023). The study by Brunner et al (2023) explored various drivers of hydrological drought in the Alps between 1970 and 2013, and revealed a diminishing trend in drought duration. Furthermore, Brunner et al (2023) highlighted an increase in the flow deficit and drought intensity, both of which were linked to snow droughts (Crausbay et al. 2020; Rhoades et al. 2022). This decrease in duration, combined with the intensification of the drought impact could also be tied to the global phenomenon of flash droughts (Yuan et al. 2023), which exhibit hotspots in the Alps and higher latitudes in Norway and Sweden. This trend is depicted in Fig. 6b, where the Hohenpeissenberg station exhibits both a general reduction in drought duration and an increase in the frequency of milder droughts (e.g. magnitude = 5), along with a slight increase in the median magnitudes.

The analysis of univariate probability distributions (illustrated in Fig. 6) provided us only limited information on how drought occurrence and frequency changed over time. For example, for the Wien station, the return period of droughts with a magnitude of 10 was reduced from 26 years (1920–1969) to 14 years (1970–2019), which does not provide us information regarding the duration of such events. At the same station and period, droughts with a duration of 5 months were also more frequent, with a return period of

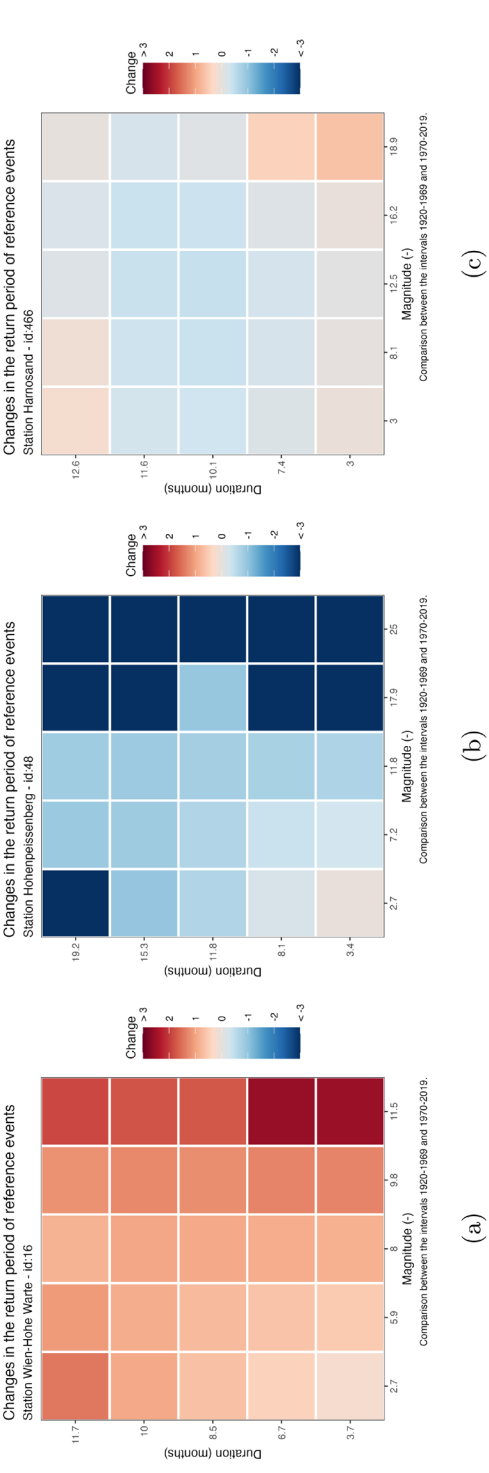

Fig. 10 Changes in the return period of specific extreme droughts in **a** Vienna (AT), **b** Hohenpeissenberg (DE), and **c** Harnosand (SE). The ratio of change is calculated by comparing the values of return periods for the reference (1920–1969) and study (1970–2019) intervals. The values of magnitude and duration on the x- and y- axis correspond to the 80th, 90th, 95th, 98th, and 99th percentile values for each variable in the reference interval. Red colours indicate an increase in the frequency (i.e. reduction in the return period).Blue colours indicate a decrease in frequency

approximatelly 4 years in 1920–1969 and of 3 years in 1970–2019. Neither of these values fully represents the actual change on droughts with magnitude of 10 and duration of 5 months, when considered the associated values in a bi-variate copula distribution. Neither of these informations fully represented the actual change on droughts with magnitude of 10 and a duration of five months when considering the associated values in a bivariate copula distribution, which have actually become more frequent by a factor of five, as illustrated in Fig. 7.

Bivariate changes cannot be as clearly perceived by analysing non-parametric or univariate distributions (Spinoni et al. 2017; Cai et al. 2021; Qiu et al. 2023), which are illustrated in the ridge plots in Fig. 6. For this task, the changes were assessed using the proposed copula-entropy drought analysis and were visualised with assistance of contour and tile plots (Fig. 4). Figures 7, 8, and 9 illustrate the changes in drought characteristics (magnitude and duration) corresponding to different frequency curves (0.2, 0.1, 0.05, and 0.02, representing return periods of 5, 10, 20, and 50 years, respectively).

The proposed copula-entropy method for studying changes in drought frequency and obtaining MDF curves (`cedaR`), as demonstrated in the three examples in Figs. 7, 8, and 9, offers a more precise and comprehensible picture of how these changes transpired and what critical extremes are emerged in each region. For instance, consider the case of a station in Potsdam (Germany), from the univariate distributions, there was evidence of an increase in the frequency of both extreme duration and magnitude; however, the precise value was hard to visualize from the ridge plots. Using the more detailed probability distribution obtained with with `cedaR` and with the contour plots, we can, for instance, say that a drought with a magnitude of 15 and a duration of 5 months, which currently has a return period of 10 years, was previously a 50-year return period event during the first half of the 20th century. This suggests a five-fold increase in the frequency of such events.

Considering the design scenarios proposed with the tile plots(Fig. 10), the station in Wien exhibited an overarching increase in the expected frequency of extreme droughts. Notably, this station exhibited a particularly pronounced surge in the frequency of droughts falling within the 0.2 frequency for duration (6.7 months) and 0.02 frequency for magnitude (11.5), located in the lower-right corner of the plot, indicating higher intensity. The frequency increase in these cases amounted to a factor of five. These results are consistent with the shifts in precipitation patterns reported by Schindler et al. (2007) and findings of Vicente-Serrano et al. (2022) concerning alterations in drought frequency within the region. In contrast, the Hohenpeissenberg station (Fig. 10b) showed a decline in the incidence of longer and higher-magnitude droughts across all scenarios. This observation aligns with the insights gained from the univariate, nonparametric probability density distributions (ridge plots—Fig. 6), which indicate a reduction in the occurrence of extreme values and an increase in mid-level droughts. This pattern was further corroborated by the bivariate analysis, as shown in Fig. 8. The alterations in both duration and magnitude were also consistent with the analyses conducted by Vicente-Serrano et al. (2022) using the SPEI. The mix-behaviour stations displayed an increase in the frequency of specific drought types (i.e., certain combinations of magnitude M and duration D), along with a decrease in others. An example of this behaviour was observed at the Harnosand Station (Fig. 10c). This station presents an increase in the frequency of very long and/or intense droughts (upper-left, upper-right, and bottom-right corners) by a factor of up to 1.5. Conversely, all other drought combinations showed a reduction in the frequency of occurrence. For a complete overview of the changes in univariate (Fig. 6), bivariate (Fig. 7, 8, and 9), and extreme event return periods (Fig. 10) across all 26 stations, detailed information is accessible in the supplements of this paper.

In this study we used a strict definition of meteorological drought (Sect. 2.2). The results presented here are intrinsically related to the selected index (SPEI3—often linked to agricultural impacts; see Mishra and Singh, 2010) and definition (after Vicente-Serrano et al. 2010 and Wang et al. 2019). The use of different indexes (Svoboda et al. 2016) and termination criteria (Parry et al. 2016) would influence the results regarding MDF curves and the changes in frequencies over time. This influence is explained by the difference in identified events according to the chosen definition (Vicente-Serrano et al. 2010; Alencar and Paton 2022). However, the copula-entropy method is consistent across different definitions criteria (e.g. Yang et al. 2021 used Hydrological Drought Index and Shekari et al. 2023 used Standard Precipitation Index) in providing reliable measures of frequency.

Finally, previous studies (Yang et al. 2021; Shekari et al. 2023; Wei and Zhao 2024) successfully implemented copula-entropy for analysing the frequency of meteorological and hydrological droughts. However, their studies were limited by the usage of considerably shorter time series and a lack of information on how drought frequency have changed in the past. Another setback of previous studies on copula-entropy drought analysis is the lack of available scripts and tools to assist in the analysis. In this study, we implemented the method of copula-entropy in R-language providing a reproducible tool to assist drought analysis. Using this new tool, it is possible to obtain not only accurate probability distributions of droughts features, but also compare the changes over the last one hundred years for multiple stations in Central Europe. Despite the limitations regarding the number and spatial distribution of the analysed stations, the availability of long and high-quality time series yielded valuable insights into changes in drought occurrences across Europe. Through the implementation of the copula-entropy analysis, we identified important zones with increases in the occurrence of extreme droughts (e.g. eastern Germany and Hungary),and areas with decreases in the incidence of such extreme events and increases in occurrence of milder/flash droughts (e.g. Alps). A notable advantage of employing such stations lies in the quality of their measurements, facilitated by consistent monitoring practices spanning over a century (Fenner et al. 2018; Paton 2022).

5 Conclusion

The use of copulas and the principle of maximum entropy is a sophisticated and efficient method for producing MDF curves of droughts. The proposed `cedaR` package does not require the testing and validation of multiple families of copulas and marginal distributions, but rather the solution of a single equation. This substantially decreases the computation time and increases the reproducibility of the method, which can be easily implemented (see the Declarations to assess the code). The copula-entropy implantation was used to analyse drought changes in Europe over the last 100 years. The changes in the MDF curves showed a heterogeneous behaviour across Europe, indicating that there was no uniform increase in frequency for all droughts, but rather different local dynamics. Therefore, the answer to the question of "which droughts are becoming more frequent" requires careful pondering. In Europe, using the most complete measured data series over the last century, we found out that, although, in general, all droughts (either extreme or mild) are more frequent, the rates of change are not the same between regions and levels of extremeness. In addition, approximately a quarter of the stations analysed showed some level of decrease in the frequency of extreme droughts, which was not necessarily accompanied by a decrease in milder droughts. Droughts will continue to bring new challenges to the societal resilience

Table 1 List of all 26 stations used in this study

Station ID	Station Name	CC	Lat	Lon	Elevation	Start	End	Annual Prec.		Annual Temp.		Change[a]
								Mean	S.D	Mean	S.D	
–	–	–	(°)		(m.a.s.l.)	year		(mm)		(°C)		(+/–)
10	STOCKHOLM	SE	59.35	18.05	44	1859	2022	555.1	92.5	7.1	1.1	+
11	KREMSMUENSTER (TAWES)	AT	48.06	14.13	382	1876	2021	1004.3	143.2	9.1	1.0	+
13	INNSBRUCK-UNIV	AT	47.26	11.38	578	1901	2021	879.9	123.0	9.7	1.0	+
15	SONNBLICK (TAWES)	AT	47.05	12.96	3109	1901	2021	1587.8	495.7	− 5.4	0.9	–
16	WIEN-HOHE WARTE	AT	48.25	16.36	198	1901	2021	648.6	109.5	10.4	1.0	+
21	ZAGREB-GRIC	HR	45.82	15.98	157	1860	2020	880.0	155.5	12.1	1.0	+
48	HOHENPEISSENBERG	DE	47.80	11.01	977	1781	2022	1163.3	170.8	7.1	0.9	–
49	JENA STERNWARTE	DE	50.93	11.58	155	1826	2022	587.6	107.9	9.7	0.9	+
54	POTSDAM	DE	52.38	13.06	81	1893	2022	586.2	100.0	9.3	0.9	+
58	ZUGSPITZE	DE	47.42	10.99	2964	1900	2022	1868.7	433.0	− 4.3	0.8	–
64	BUDAPEST	HU	47.51	19.02	153	1901	2020	579.2	122.3	11.8	0.9	+
162	DE BILT-1	NL	52.10	5.18	2	1905	2022	798.7	139.7	9.6	0.9	+/–
164	GRONINGEN-1	NL	53.18	6.60	1	1846	2022	775.3	114.5	8.8	0.9	+/–
239	BASEL BINNINGEN	CH	47.53	7.58	316	1901	2022	801.1	141.8	10.5	0.8	–
242	LUGANO	CH	46.00	8.97	273	1901	2022	1647.7	348.3	12.6	0.7	+/–
243	SAENTIS	CH	47.25	9.35	2502	1901	2022	2646.7	610.2	− 1.4	0.9	+
244	ZUERICH/FLUNTERN	CH	47.38	8.57	555	1901	2022	1098.2	174.0	9.7	0.7	–
324	LINDENBERG	DE	52.21	14.12	98	1906	2022	559.8	100.4	9.1	1.0	+/–
466	HARNOSAND	SE	62.63	17.93	15	1868	2022	704.8	128.9	4.4	1.1	+/–
786	MONTELIMAR	FR	44.58	4.73	73	1920	2020	940.4	230.8	13.4	0.8	+
849	PECS POGANY	HU	46.01	18.23	203	1901	2020	652.0	129.2	11.2	0.8	+/–
851	SZEGED	HU	46.26	20.09	82	1901	2020	531.9	121.9	11.3	0.9	+
852	DEBRECEN AIRPORT	HU	47.49	21.61	108	1901	2020	561.5	117.1	10.4	0.9	+
1422	BORAS	SE	57.76	12.95	135	1884	2022	979.0	169.8	6.5	1.0	–

Table 1 (continued)

Station ID	Station Name	CC	Lat	Lon	Elevation	Start	End	Annual Prec.		Annual Temp.		Change[a]
								Mean	S.D	Mean	S.D	
–	–	–	(°)		(m.a.s.l.)	year		(mm)		(°C)		(+/–)
2042	SZOMBATHELY	HU	47.20	16.65	201	1901	2020	614.6	103.8	9.9	0.9	+
4002	OBERSTDORF	DE	47.40	10.28	806	1910	2022	1763.1	249.5	6.9	0.8	+

[a]Stations marked in + (–) had an overall increase (decrease) in the frequency of extreme events. Two signs indicate a more intense change

All stations satisfy the two criteria described on the paper. CC is the two digit country code

and sustainability as human-induced climate change intensifies. The results and methodology of this study provide actionable knowledge and reproducible tools for obtaining and updating expected droughts and their probabilities.

Appendix A. Selected stations

See Table 1.

Supplementary Information The online version contains supplementary material available at https://doi.org/10.1007/s11069-024-06848-y.

Acknowledgements This research was funded through by the Einstein Research Unit "Climate and Water under Change" of the Einstein Foundation Berlin and Berlin University Alliance (ERU-2020-609).

Author contributions PHLA was responsible by conceptualization, data acquisition, processing, and analysis, script and manuscript writing. ENP contributed with data analysis and manuscript writing.

Funding Open Access funding enabled and organized by Projekt DEAL. This study was funded by the Einstein Research Unit 'Climate and Water under Change' of the Einstein Foundation Berlin and the Berlin University Alliance (ERU-2020-609).

Data availability All data and metadata used in this study are publicly available at https://www.ecad.eu. Data and materials are also available upon request.

Code availability All code is available at https://github.com/pedroalencar1/cedaR.

Declarations

Conflict of interest The authors have no Conflict of interest

References

AghaKouchak A (2014) Entropy–copula in hydrology and climatology. J Hydrometeorol 15(6):2176–2189. https://doi.org/10.1175/jhm-d-13-0207.1

AghaKouchak A, Mirchi A, Madani K et al (2021) Anthropogenic drought: definition, challenges, and opportunities. Rev Geophys. https://doi.org/10.1029/2019rg000683

Alencar PHL (2023) Droughtsdf: R-package and matlab workflow to estimate severity-duration-frequency curves. https://doi.org/10.5281/ZENODO.7926210

Alencar PHL, Paton EN (2022) How do we identify flash droughts? A case study in central European croplands. Hydrol Res 53(9):1150–1165. https://doi.org/10.2166/nh.2022.003

Alencar PHL, Paton EN, de Araújo JC (2021) Entropy-based temporal downscaling of precipitation as tool for sediment delivery ratio assessment. Entropy. https://doi.org/10.3390/e23121615

Ayantobo OO, Li Y, Song S (2018) Multivariate drought frequency analysis using four-variate symmetric and asymmetric Archimedean copula functions. Water Resour Manag 33(1):103–127. https://doi.org/10.1007/s11269-018-2090-6

Bevacqua E, Maraun D, Haff IH et al (2017) Multivariate statistical modelling of compound events via pair-copula constructions: analysis of floods in Ravenna (Italy). Hydrol Earth Syst Sci 21(6):2701–2723. https://doi.org/10.5194/hess-21-2701-2017

Brunner MI, Götte J, Schlemper C et al (2023) Hydrological drought generation processes and severity are changing in the alps. Geophys Res Lett. https://doi.org/10.1029/2022gl101776

Cai S, Song X, Hu R et al (2021) Spatiotemporal characteristics of agricultural droughts based on soil moisture data in inner Mongolia from 1981 to 2019. J Hydrol 603(127):104. https://doi.org/10.1016/j.jhydrol.2021.127104

Chu B, Satchell S (2018) The most entropic canonical copula with an application to 'style' investment. Asymmetric dependence in finance: diversification, correlation and portfolio management in market downturns. Wiley, Hoboken, pp 221–262

Cook BI, Cook ER, Smerdon JE et al (2016) North American megadroughts in the common era: reconstructions and simulations. WIREs Clim Change 7(3):411–432. https://doi.org/10.1002/wcc.394

Cover TM, Thomas JA (2006) Elements of information theory. John Wiley & Sons, Hoboken

Crausbay SD, Betancourt J, Bradford J et al (2020) Unfamiliar territory: emerging themes for ecological drought research and management. One Earth 3(3):337–353. https://doi.org/10.1016/j.oneear.2020.08.019

Cravens AE, Henderson J, Friedman J et al (2021) A typology of drought decision making: synthesizing across cases to understand drought preparedness and response actions. Weather Clim Extrem 33(100):362. https://doi.org/10.1016/j.wace.2021.100362

Fenner D, Holtmann A, Krug A et al (2018) Heat waves in berlin and Potsdam, Germany—long-term trends and comparison of heat wave definitions from 1893 to 2017. Int J Climatol 39(4):2422–2437. https://doi.org/10.1002/joc.5962

Gül GO, Gül A, Najar M (2021) Historical evidence of climate change impact on drought outlook in river basins: analysis of annual maximum drought severities through daily SPI definitions. Nat Hazards 110(2):1389–1404. https://doi.org/10.1007/s11069-021-04995-0

Hasan IF, Abdullah R (2022) Agricultural drought characteristics analysis using copula. Water Resour Manag 36(15):5915–5930. https://doi.org/10.1007/s11269-022-03331-w

Hofert M, Kojadinovic I, Mächler M et al (2019) Elements of copula modeling with R. Springer-Verlag GmbH, Berlin

Houmma IH, Mansouri LE, Gadal S et al (2022) Modelling agricultural drought: a review of latest advances in big data technologies. Geomat Nat Hazard Risk 13(1):2737–2776. https://doi.org/10.1080/19475705.2022.2131471

IPCC (2023) Climate change 2023: synthesis report—a report of the intergovernmental panel on climate change. Contribution of Working Groups I, II and III to the Sixth Assessment Report of the Intergovernmental Panel on Climate Change [Core Writing Team, H. Lee and J. Romero (eds.)], Geneva, Switzerland

Jaynes ET (1957) Information theory and statistical mechanics. Phys Rev 106(4):620–630. https://doi.org/10.1103/physrev.106.620

Jaynes ET (1957) Information theory and statistical mechanics II. Phys Rev 108(2):171–190. https://doi.org/10.1103/physrev.108.171

Jeffreys H (2000) Theory of probability Clarendon Press, 3rd edn. Oxford University Press, Oxford

Lagarias JC, Reeds JA, Wright MH et al (1998) Convergence properties of the Nelder–Mead simplex method in low dimensions. SIAM J Optim 9:112–147

Lloyd-Hughes B (2013) The impracticality of a universal drought definition. Theor Appl Climatol 117(3–4):607–611. https://doi.org/10.1007/s00704-013-1025-7

Loon AFV, Gleeson T, Clark J et al (2016) Drought in the Anthropocene. Nat Geosci 9(2):89–91. https://doi.org/10.1038/ngeo2646

Mikosch T (2006) Copulas: tales and facts. Extremes 9(1):3–20. https://doi.org/10.1007/s10687-006-0015-x

Mirschel W, Wieland R, Luzi K et al (2020) Model-based estimation of irrigation water demand for different agricultural crops under climate change, presented for the federal state of Brandenburg, Germany. Innovations in landscape research. Springer International Publishing, Berlin, pp 311–327

Mishra AK, Singh VP (2010) A review of drought concepts. J Hydrol 391(1–2):202–216. https://doi.org/10.1016/j.jhydrol.2010.07.012

Mohammed S, Alsafadi K, Enaruvbe GO et al (2022) Assessing the impacts of agricultural drought (SPI/SPEI) on maize and wheat yields across Hungary. Sci Rep. https://doi.org/10.1038/s41598-022-12799-w

Mote PW, Allen MR, Jones RG et al (2016) Superensemble regional climate modeling for the western United States. Bull Am Meteorol Soc 97(2):203–215. https://doi.org/10.1175/BAMS-D-14-00090.1

Nelsen RB (2007) An introduction to copulas. Springer-Verlag GmbH, Berlin

Noguera I, Domínguez-Castro F, Vicente-Serrano SM (2020) Characteristics and trends of flash droughts in Spain, 1961–2018. Ann N Y Acad Sci 1472(1):155–172

Pandey V, Pandey PK, Lalrammawii H (2023) Characterization and return period analysis of meteorological drought under the humid subtropical climate of manipur, northeast india. Nat Hazards Res. https://doi.org/10.1016/j.nhres.2023.07.007

Parry S, Prudhomme C, Wilby RL et al (2016) Drought termination: concept and characterisation. Prog Phys Geogr Earth Environ 40(6):743–767. https://doi.org/10.1177/0309133316652801

Paton E (2022) Intermittency analysis of dry spell magnitude and timing using different spell definitions. J Hydrol 608(127):645. https://doi.org/10.1016/j.jhydrol.2022.127645

Qi Y, Yu H, Fu Q et al (2022) Future changes in drought frequency due to changes in the mean and shape of the PDSI probability density function under RCP4.5 scenario. Front Earth Sci. https://doi.org/10.3389/feart.2022.857885

Qiu J, Shen Z, Xie H (2023) Drought impacts on hydrology and water quality under climate change. Sci Total Environ 858(159):854. https://doi.org/10.1016/j.scitotenv.2022.159854

Rhoades AM, Hatchett BJ, Risser MD et al (2022) Asymmetric emergence of low-to-no snow in the midlatitudes of the American Cordillera. Nat Clim Change 12(12):1151–1159. https://doi.org/10.1038/s41558-022-01518-y

Rubel F, Kottek M (2010) Observed and projected climate shifts 1901–2100 depicted by world maps of the Köppen-Geiger climate classification. Meteorol Z 19(2):135–141. https://doi.org/10.1127/0941-2948/2010/0430

Schindler U, Steidl J, Müller L et al (2007) Drought risk to agricultural land in northeast and central Germany. J Plant Nutr Soil Sci 170(3):357–362

She D, Mishra AK, Xia J et al (2015) Wet and dry spell analysis using copulas. Int J Climatol 36(1):476–491. https://doi.org/10.1002/joc.4369

Sheffield J, Wood EF, Roderick ML (2012) Little change in global drought over the past 60 years. Nature 491(7424):435–438. https://doi.org/10.1038/nature11575

Shekari M, Zamani H, Bazrafshan O et al (2023) Maximum entropy copula for bivariate drought analysis. Phys Chem Earth Parts ABC 131(103):419. https://doi.org/10.1016/j.pce.2023.103419

Singh VP (1998) Entropy-based parameter estimation in hydrology. Springer, Dordrecht

Singh VP, Zhang L (2018) Copula—entropy theory for multivariate stochastic modeling in water engineering. Geosci Lett. https://doi.org/10.1186/s40562-018-0105-z

Sklar M (1959) Fonctions de repartition an dimensions et leurs marges. Publ Inst Statist Univ Paris 8:229–231

Spinoni J, Vogt JV, Naumann G et al (2017) Will drought events become more frequent and severe in Europe? Int J Climatol 38(4):1718–1736. https://doi.org/10.1002/joc.5291

Svoboda M, LeComte D, Hayes M et al (2002) The drought monitor. Bull Am Meteor Soc 83(8):1181–1190. https://doi.org/10.1175/1520-0477-83.8.1181

Svoboda MD, Fuchs BA et al (2016) Handbook of drought indicators and indices. World Meteorological Organization Geneva, Switzerland

Tank AMGK, Wijngaard JB, Können GP et al (2002) Daily dataset of 20th-century surface air temperature and precipitation series for the European climate assessment. Int J Climatol 22(12):1441–1453. https://doi.org/10.1002/joc.773

Teutschbein C, Jonsson E, Todorović A et al (2023) Future drought propagation through the water-energy-food-ecosystem nexus—a Nordic perspective. J Hydrol 617(128):963. https://doi.org/10.1016/j.jhydrol.2022.128963

Thiery W, Lange S, Rogelj J et al (2021) Intergenerational inequities in exposure to climate extremes. Science 374(6564):158–160. https://doi.org/10.1126/science.abi7339

Tosunoglu F, Can I (2016) Application of copulas for regional bivariate frequency analysis of meteorological droughts in Turkey. Nat Hazards 82(3):1457–1477. https://doi.org/10.1007/s11069-016-2253-9

Vicente-Serrano SM, Begueria S, López-Moreno JI (2010) A multiscalar drought index sensitive to global warming: the standardized precipitation evapotranspiration index. J Clim 23(7):1696–1718. https://doi.org/10.1175/2009jcli2909.1

Vicente-Serrano SM, Peña-Angulo D, Beguería S et al (2022) Global drought trends and future projections. Philos Trans R Soc Math Phys Eng Sci 380(2238):200. https://doi.org/10.1098/rsta.2021.0285

Wang F, Wang Z, Yang H et al (2019) Copula-based drought analysis using standardized precipitation evapotranspiration index: a case study in the yellow river basin, china. Water 11(6):1298. https://doi.org/10.3390/w11061298

Wang M, Liu M, Zhang D et al (2023) Assessing and optimizing the hydrological performance of grey-green infrastructure systems in response to climate change and non-stationary time series. Water Res 232(119):720. https://doi.org/10.1016/j.watres.2023.119720

Wei T, Zhao X (2024) Assessment of spatial-temporal variation of precipitation and meteorological drought in Shanxi province, China. Nat Hazards 120(6):5579–5599. https://doi.org/10.1007/s11069-024-06430-6

WMO (1992) International meteorological vocabulary, 2nd edn. World Meteorological Organization (WMO)

Wuebbles D, Easterling D, Hayhoe K et al (2017) Ch. 1: Our globally changing climate. In: Climate science special report: fourth national climate assessment, vol i. Tech. rep., U.S. Global Change Research Program. https://doi.org/10.7930/j08s4n35

Xu C, McDowell NG, Fisher RA et al (2019) Increasing impacts of extreme droughts on vegetation productivity under climate change. Nat Clim Change 9(12):948–953. https://doi.org/10.1038/s41558-019-0630-6

Xu K, Yang D, Xu X et al (2015) Copula based drought frequency analysis considering the spatio-temporal variability in southwest China. J Hydrol 527:630–640. https://doi.org/10.1016/j.jhydrol.2015.05.030

Yang X, Li YP, Huang GH (2021) A maximum entropy copula-based frequency analysis method for assessing bivariate drought risk: a case study of the kaidu river basin. J Water Clim Change 13(1):175–189. https://doi.org/10.2166/wcc.2021.272

Yuan X, Wang Y, Ji P et al (2023) A global transition to flash droughts under climate change. Science 380(6641):187–191. https://doi.org/10.1126/science.abn6301

Zhang L, Singh V (2019) Copulas and their applications in water resources engineering. Cambridge University Press, Cambridge

Zink M, Samaniego L, Kumar R et al (2016) The German drought monitor. Environ Res Lett 11(7):074002

Zscheischler J, van den Hurk B, Ward PJ et al (2020) Multivariate extremes and compound events. Climate extremes and their implications for impact and risk assessment. Elsevier, Amsterdam, pp 59–76